3D-Printed Microfluidic Chip System for Dielectrophoretic Manipulation of Colloids

N. Philippin[1], A. Frey[2], M. Michatz[2] and I. Kuehne[1]*
[1] Heilbronn University of Applied Sciences, Kuenzelsau, BW, Germany
[2] University of Applied Sciences, Augsburg, BY, Germany
*Corresponding author: ingo.kuehne@hs-heilbronn.de

Abstract – The capability to manipulate colloids down to microscopical levels, paves the way for revolutionary applications in medical science and technology. In that context, the present analysis investigates the electrokinetic phenomenon of dielectrophoresis (DEP) as effective technique for manipulation of particles within an additive manufactured microfluidic chip system. The results, arised from COMSOL Multiphysics simulations, are used to provide evidence for optimizing the prototype concerning a most suitable positioning of electrodes inside the device as well as the applied voltage to generate a non-uniform electric field, which is a mandatory requirement to realise DEP.

Keywords: electrokinetics, microfluidics, dielectrophoresis, particle manipulation, 3D-printing, FEM

1. Introduction

Microfluidics, as a crucial technology of recent years, enables numerous applications for Point-of-Care-Testing such as Lab-on-Chip-Systems (LOC) or Micro-Total-Analysis-Systems (µTAS) and is exceptionally well-suited for cell sorting or DNA trapping. Notably a range of electrokinetic phenomena, e.g. electrophoresis, dielectrophoresis or electroosmosis, plays a pivotal role for the conception of microfluidic systems. Especially the implementation of dielectrophoresis (DEP) in microfluidic chips has evolved to a subtle method for precise manipulation of appropriate cells, molecules or particles [1,2]. DEP is based on the movement of particles in a non-uniform electric field due to the interaction between the dipole of the particle and the spatial gradient of the electric field. Thereby, the generated dielectrophoretic force depends on two main parameters, the particle size and the electrical properties of the suspending medium [3,4]. In this context, the aforementioned force is responsible for deflection of particles in microfluidic channels and leads to characteristic trajectories of the colloids within these filigree structures [5]. Contrary to conventional production methods, additive manufacturing, also known as 3D-printing, allows the generation of sophisticated microscale geometries and represents a relatively simple, inexpensive and long-term alternative for prospective production of such systems [6].

2. Fundamentals of dielectrophoresis

Dielectrophoretic processes in microfluidic systems emerge from polarizable particles, which are suspended to a non-uniform electric field. DEP involves, compared to other common methods, several advantages that encourage particle movement in microchannels [7]:

- DEP is applicable for both, conducting and non-conducting particles.
- The non-uniform electric field can be created either by applying alternating current (AC) or direct current (DC).
- Possibility to generate positive and negative forces.
- DEP shows beneficial scaling effects.

2.1. Dipole moment & dielectrophoretic force

As indicated, one of the main benefits of DEP is the fact, that both, AC- or DC-fields, can be used for the realisation of this electrokinetic phenomenon. Thus, the following specifications refer to the implementation of DEP via AC-fields as common method. In case of using DC-fields like in the present study, the theoretical background can be assumed as approximation on low frequency AC-fields. Relevant deviations will be explained at regarding situations [7].

For improved understanding of DEP, it is useful to distinguish the behaviour of particles in uniform as well as non-uniform electric fields. In the first case, differences regarding the migration of charged and neutral particles can be observed. A charged particle

subjected to a uniform AC-field experiences a net force, which results in a movement. In contrast, neutral particles emerge a zero net force because charges are equal on both sides of the particle and counteract each other. A descriptive illustration can be found in Fig. 1.

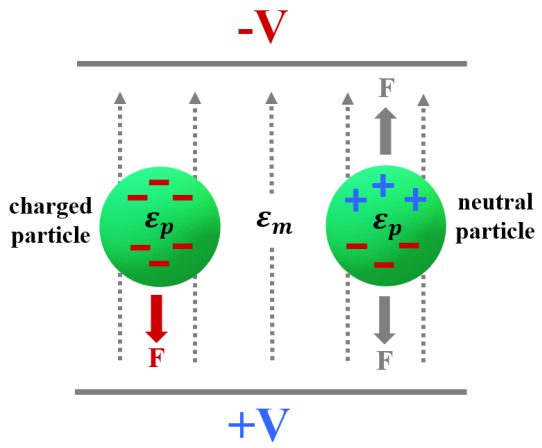

Figure 1. Movement of charged and neutral particles in a uniform electric field: net force and resulting migration of charged particle (left); counteracting forces without any resulting migration of a neutral particle (right).

As soon as a neutral particle is located within an inhomogeneous electric field, however, a dipole and a net force will be formed, which results in attraction and repulsion of the spheres. The induced dipole moment of a spherical particle with radius r corresponds to overall polarisation of it. If the particle undergoes a sinusoidal amplitude ($E_{el.}\, sin(\omega t)$), the dipole moment p^* can be described, depending on the permittivity of the suspending medium ε_m, the real part of the Clausius-Mossotti-Factor f_{CM} and the root mean square amplitude of the electric field E_{rms}, by the following equation:

$$p^* = 4\pi\varepsilon_m \Re[f_{CM}(\omega)] r^3 E_{rms} \qquad (1)$$

The accumulation of charges, that interact between the suspending medium and the particle leads to an unequal force, the so called dielectrophoretic force F_{DEP}, whose magnitude and orientation depends on the electric properties of particle and medium. The dielectrophoretic force F_{DEP} follows the notation below:

$$F_{DEP} = 2\pi r^3 \varepsilon_0 \varepsilon_m \Re[f_{CM}(\omega)] \nabla E_{rms}^2 \qquad (2)$$

with the spatial gradient of the non-uniform electric field ∇E_{rms}^2 and the permittivity of the vacuum ε_0. The dielectrophoretic force can be characterised by the subsequent aspects [7]:

- F_{DEP} solely exists in combination with non-uniform electric fields.
- F_{DEP} is proportional to permittivity of particle and medium.
- F_{DEP} is dependent on the magnitude of the Clausius-Mossotti-Factor.
- F_{DEP} is regardless of the field polarity.
- F_{DEP} is proportional to the particles volume.

2.2. Clausius-Mossotti-Factor

To consider frequency dependence, the complex permittivities of both, medium (ε_m^*) and particle (ε_p^*) as well as the angular frequency ω, are integrated over the Clausius-Mossotti-Factor $f_{CM}(\omega)$. The Clausius-Mossotti-Factor reflects the extent of particle polarisation and is given by:

$$f_{CM}(\omega) = \frac{\varepsilon_p^* - \varepsilon_m^*}{\varepsilon_p^* - 2\varepsilon_m^*} \qquad (3)$$

whereby the complex permittivities can be also expressed as $\varepsilon_m^* = \varepsilon_m - j\frac{\sigma_m}{\omega}$ or rather $\varepsilon_p^* = \varepsilon_p - j\frac{\sigma_p}{\omega}$. Whereas the dielectrophoretic force F_{DEP} remains unchanged regardless of applying AC or DC-fields, the Clausius-Mossotti-Factor considers DC-fields via following equation:

$$f_{CM}(\sigma_p, \sigma_m) = \frac{\sigma_p - \sigma_m}{\sigma_p - 2\sigma_m} \qquad (4)$$

with the conductivities of the medium σ_m and the particle σ_p. Subsequently, a compartmentation of real part and imaginary part pursuant to equation (3) leads to the following expressions [8]:

$$\Re[f_{CM}(\omega)] = \frac{\omega^2(\varepsilon_p - \varepsilon_m)(\varepsilon_p + 2\varepsilon_m) + (\sigma_p - \sigma_m)(\sigma_p + 2\sigma_m)}{\omega^2(\varepsilon_p + 2\varepsilon_m)^2 + (\sigma_p + 2\sigma_m)^2} \qquad (5)$$

and

$$\Im[f_{CM}(\omega)] = \frac{\omega(\sigma_m - \sigma_p)(\varepsilon_p + 2\varepsilon_m) - (\varepsilon_p - \varepsilon_m)(\sigma_p + 2\sigma_m)}{\omega^2(\varepsilon_p + 2\varepsilon_m)^2 + (\sigma_p + 2\sigma_m)^2} \qquad (6)$$

Notably the real part of the Clausius-Mossotti-Factor $\Re[f_{CM}(\omega)]$ is decisive for dielectrophoresis and responsible for the direction of particle movement. As a result of the real part, two principles of DEP arise, the positive dielectrophoresis (pDEP) and the negative dielectrophoresis (nDEP). If the polarizability of

the particle is greater than the polarizability of the medium ($\Re[f_{CM}(\omega)] > 0$), pDEP occurs. Thereby, the net force points to the direction of the field gradient and the particle will be pushed towards areas of distinct electric fields. On the other hand, if the polarizability of the particle is lower than the polarizability of the medium ($\Re[f_{CM}(\omega)] < 0$), the particle emerges a repulsion contrary to sections of strong electric fields. This principle is called nDEP (cf. Fig. 2) [9].

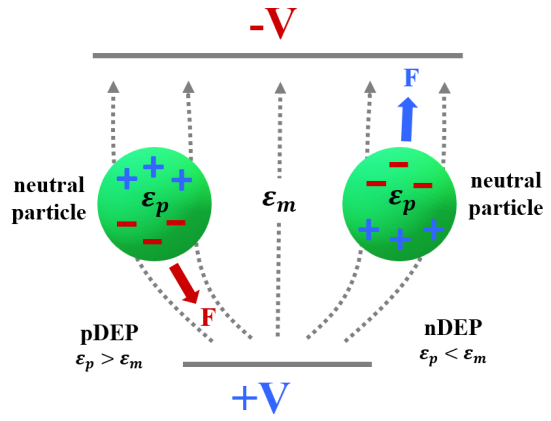

Figure 2. DEP in a non-uniform electric field: positive DEP (left) and negative DEP (right).

3. Chip design

For the purpose of substantiating the results of the COMSOL Multiphysics simulations, an additive manufactured prototype, adapted to the 2D-channel-geometry of the FEM-model, was designed and printed via MultiJet Modeling (MJM). Additive production methods like MJM are well-suited to generate filigree structures without major efforts. They even allow the use of biocompatible materials suitable for medical applications such as LOC or µTAS [10]. Hence, the printed chip system was used for characterisation not solely due to FEM-simulations but rather for practical test series to confirm the functionality of the microfluidic chip especially under real conditions (cf. section 5).

3.1. Geometrical aspects

Centrepiece of the printed prototype is the micro-scaled channel system with respectively two inflow- and two outflow-branches and one separation channel to realise the non-uniform electric field. The symmetrically configured elements ensure a monitored flow of particles as well as the electrolyte solution. Thus, reproductible results are achievable. Figure 3 depicts the fundamental geometry of the chip. Whereas Fig. 3 a) shows a corresponding CAD-model, part b) illustrates the manufactured chip. A photopolymer called VisiJet M3 Crystal was used as building material. The inflow and outflow branches have a diameter of 500 µm and the separation channel of 1000 µm to achieve a homogeneous influx of particles, while the length of the separation channel is designed with 40 mm. For the sake of simplicity, the 2D-model for purpose of FEM-simulations, has been shortened to 20 mm, which does not lead to any restrictions regarding the obtained results.

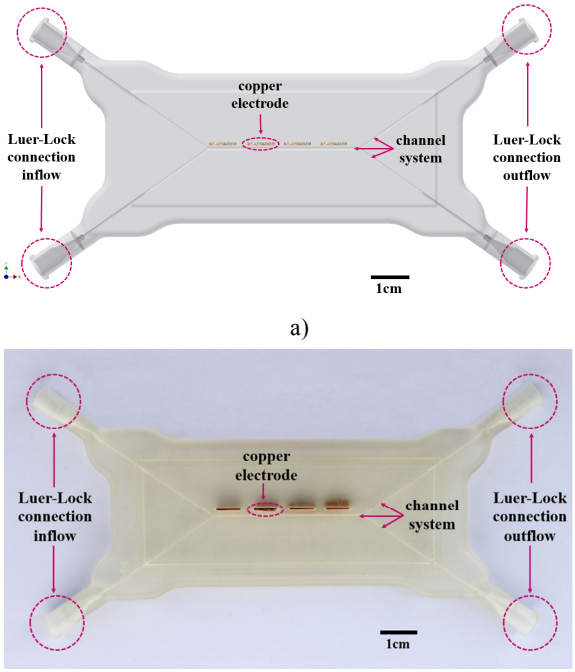

Figure 3. a) CAD-model of the microfluidic chip system, b) 3D-printed prototype (material: VisiJet M3 Crystal).

3.2. Luer-Lock connection system

To enable a simple process handling, a so-called Luer-Lock system was implemented into the chip (cf. Fig. 3 and 4). Luer-Lock connections are subjected to the standardized norm EN ISO 80369-7: 2016 and well established on the market for medical devices since several years [11]. Via screw connections, tubes of various diameters can be coupled with each other. The female Luer element consists of a kind of hollow cylinder with external wings. The antagonistical part, the male Lock connection, can be bolt very tight to avoid air pockets within the channel during process flow. This technique offers great potentials for future applications in medical sciences to connect inter alia tubes, micro pumps or syringes for accurate dosing of liquids or colloids. A close-up of the Luer-Lock connection can be inferred from Fig. 4. Clearly visible are the zirconium oxide particles (whitish structure)

within the connected silicone tube used for the feasibility study with diameters between 30 µm and 60 µm.

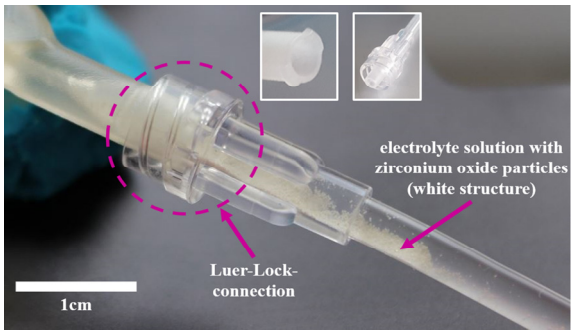

Figure 4. Luer-Lock connection of the chip system for simple process handling.

4. Use of COMSOL Multiphysics®

The COMSOL Multiphysics® model is set up with the Electrostatics interface, the Laminar Flow interface as well as the Particle Tracing module. For numeric efficiency, a 2D geometry of the previously presented microchannel system is established in order to simulate the targeted deflection of zirconium oxide particles due to the dielectrophoretic force F_{DEP} caused by an electric DC-field. To pursue the goal of optimizing the position of copper electrodes inside the microfluidic chip system and the applied voltage for the generation of a non-uniform electric DC-filed, some settings are necessary to achieve comprehensible results. Table 1 gives an overview concerning the most relevant parameters and values adjusted in context with the simulation of DEP.

Table 1. Parameters settings. Water serves as electrolyte solution and particles consist of zirconium oxide.

parameter	value	unit
dynamic viscosity water $\boldsymbol{\mu_m}$	$10002 \cdot 10^{-6}$	Pa*s
density water $\boldsymbol{\rho_m}$	998,21	kg/m^3
density particle $\boldsymbol{\rho_p}$	5680	kg/m^3
particle diameter	30-45	µm
electrical conductivity water $\boldsymbol{\sigma_m}$	$5{,}5 \cdot 10^{-6}$	S/m
permittivity vacuum $\boldsymbol{\varepsilon_0}$	$8{,}854 \cdot 10^{-12}$	C/Vm
relative permittivity water $\boldsymbol{\varepsilon_{rm}}$	80	-
relative permittivity particle $\boldsymbol{\varepsilon_{rp}}$	7,5	-
temperature	293,15	K
pressure inflow	0,5	Pa

4.1. Configuration of electrodes

One fundamental objective of the present paper is the optimisation of DEP within the microfluidic chip system due to the appropriate arrangement of copper electrodes. Thus, five different configurations were tested. Figure 5 a)-e) illustrates the varied positioning of the electrodes. Case a) shows an alternating and overlapping arrangement of electrodes. It is evident, that all particles pass the upper outflow branch. This situation is caused by the compensation of the generated DC-field over the entire channel length. Merely the last pair of electrodes forms a relatively low DEP which leads to the deflection of particles towards the upper branch. It can be assumed that arrangement a) does not yield reliable results in any case. Therefore, it is out of the question. A parallel alignment of electrode pairs in Fig. 5 b) with alternating voltage shows a similar result. All particles are deflected towards the upper outflow branch. In contrast to the first case, an utter focussing of the particles in the middle of the separation channel can be observed. Hence, it can be expected that the colloids are randomly deflected due to the numeric of FEM. A modification of the mesh can just as well provide opposite findings. Furthermore, it can be observed that a parallel configuration results in strong acceleration or rather deceleration of particles by entering or leaving the electric DC-field. Consequence is a significant enlargement of processing times.

In addition, redundancies can be monitored in context with variant c). A repeated parallel arrangement of electrodes (here, opposite electrodes have the same voltage) leads to a symmetrical flow profile as well as a distinct focussing of the particles within the separation channel. No deflection can be registered what results in a confluence of particle into both outflow branches. Thus, DEP cannot be verified. The experience from previous experiments has shown that a double-sided configuration of electrodes will not be crowned by success. So, case d) shows the biased positioning of electrodes. For the first time, an asymmetrical flow profile can be observed. The noticeable shift in a vertical direction leads to characteristic trajectories of the colloids caused by the dielectrophoretic force. With the final configuration e) a combination of variant b) and d) was tested out. At the beginning, pairs of electrodes are responsible for a focussed movement of particles. Because of the biased arrangement at the end of the channel, a deflection in vertical direction can be achieved as well as the DEP.

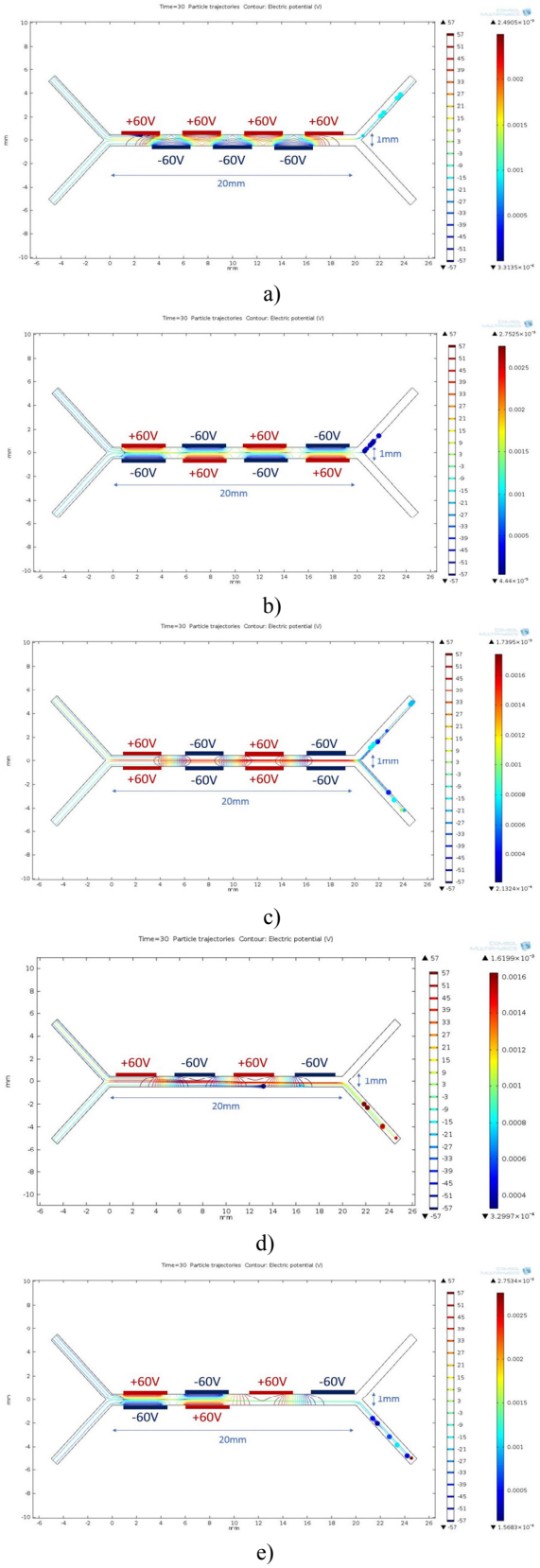

Figure 5. Electrode configurations: a) alternating and overlapping arrangement b) parallel alignment of electrode pairs, alternating voltage c) parallel alignment of electrode pairs, pairings with identical voltage d) biased configuration, alternating sign and e) combination of b) and d).

It can be summarized, that, according to the results of all COMSOL Multiphysics simulations, the configuration of electrodes in microfluidic systems plays a significant role for the successful realisation of DEP. Solely, model d) and e) can achieve reliable results. Table 2 illustrates all relevant results in a compressed form. Based on the findings above, the prototype was realised analogous to configuration d) as less sophisticated solution.

Table 2. Summary of the simulation results for various electrode configurations obtained with COMSOL Multiphysics®.

configuration	evidence DEP	deceleration/ acceleration of particles	flow profile
a)	no	low	symmetrical
b)	no	significant	symmetrical
c)	no	weak	symmetrical
d)	yes	low	asymmetrical
e)	yes	significant	asymmetrical

4.2. Impact of scaling the applied voltage

The simulation results have shown that DEP can be significantly controlled over the arrangement of electrodes within the system. Another aspect that should be mentioned is the influence of the applied voltage. The strength of the electric field affects the deflection, acceleration and deceleration of zirconium oxide particles demonstrably.

Therefore, the applied voltage of configuration d) was scaled-up stepwise from the value +/- 40V to +/- 80V. Figure 6 illustrates the corresponding simulation results. Quintessence of this test is the fact, that there is a threshold, which must be exceeded to generate reliable results. In case of applying +/- 40 V, Fig. 6 a) proves that the electric DC-field is not strong enough to form a dielectrophoretic force. The path of all particles runs almost horizontal what leads to a split of trajectories at the end of the separation channel.

An increase of the value up to +/-50 V provides interesting findings. Obviously, the threshold is reached at this point. The desired deflection of particles is realised as well as the formation of the dielectrophoretic force what can be recognized by arrowheads on the particles in Fig. 6 b). Similar results can be achieved via applying +/- 60 V (cf. Fig. 6 c)). This value has

proven to be an effective setting for successful DEP with fast processing times due to the balanced relationship between deflection, acceleration and deceleration. The F_{DEP} is strong enough to influence the movement of the particles at this point. Furthermore, they do not impede each other because of moderate repulsion by applying +/- 60 V. A last test was carried out by scaling up the voltage to +/- 80 V. As already suspected, this value entails a distinct influence of the particle movement and is responsible for a mutual obstruction of the process flow caused by collisions of particles due to the strong electric DC-field.

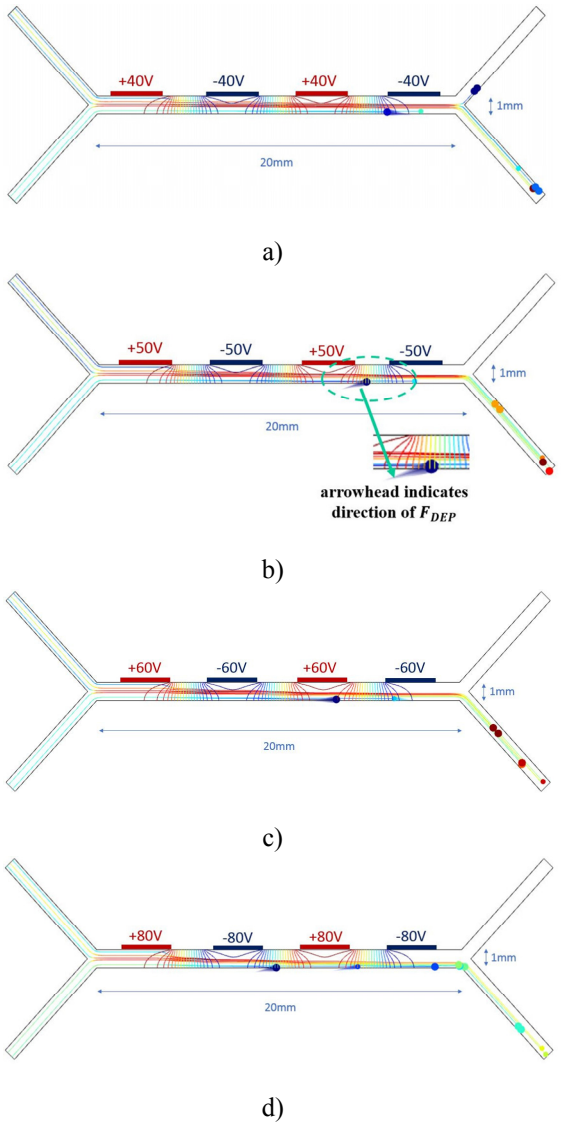

Figure 6. Impact of scaling the voltage: a) +/- 40 V: strength of electric DC-field is low, no adequate deflection of particles, outflow over both branches; b) +/- 50 V: deflection is more powerful, DEP feasible; c) +/- 60 V: pronounced deviation of particles; short processing time d) +/- 80 V: strong deflection of particles as well as acceleration and deceleration of them.

5. Results of practical experiments

As mentioned before, the 3D-printed microfluidic chip system was used to investigate the electrokinetic phenomenon under real conditions. Thus, an experimental setup consists of a digital microscope, the chip system with connectors, tubes, power supplies, a multimeter to control the process parameters, a monitor to observe and evaluate the pictures and micropumps for infiltrating the electrolyte solution as well as the zirconium oxide particles was realised. Figure 7 shows some film sequences to exemplarily depict the characteristic trajectory of a particle under the influence of a non-uniform electric DC-field and the corresponding dielectrophoretic force.

Whereas the particle passes the separation channel due to the electric DC-field towards the two outflow branches (cf. Fig. 7 a) + b)), the film sequences of Fig. 7 c) to 7 e) show the deflection into the lower outflow branch until the Luer-Lock connection. Collectively, Fig. 7 f) superimposes part a) – e). Hereby, the achieved result confirms the functionality of the microfluidic chip system and substantiates the presented findings of the FEM simulations.

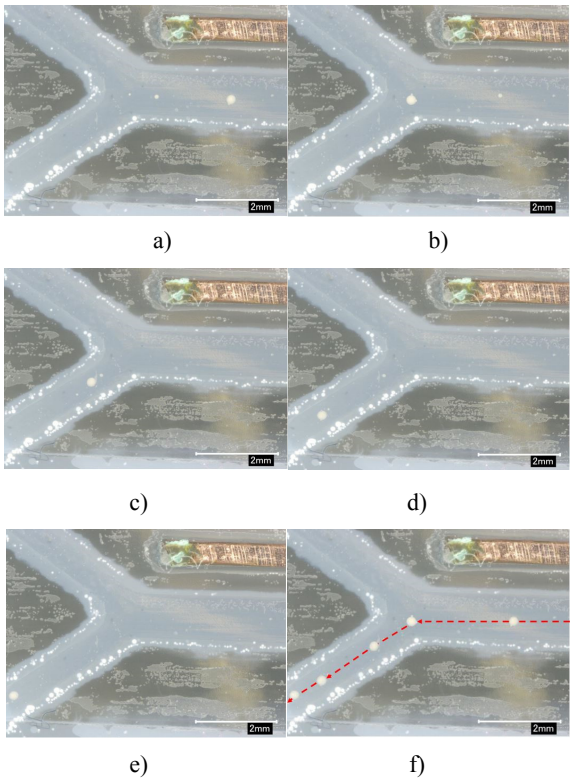

Figure 7. Images generated by digital microscope: a) particle passes separation channel due to the F_{DEP}; b) particle flows towards the lower outflow branch; c) + d) + e) until the Luer-Lock connector is reached; f) superimposition of picture a)-e) to clarify the typical particle trajectory.

6. Conclusions and outlook

A COMSOL Multiphysics model of a microfluidic chip system for dielectrophoretic manipulation of colloids was successfully established. In this context, an optimised arrangement of copper electrodes to generate a mandatory electric DC-field was found as well as a threshold, which must be exceeded to generate reliable results.

Moreover, predictions can be done regarding the conceptions of prospective microfluidic devices. Especially the miniaturisation of such systems should be considered.

In case of the presented analysis and the fabrication of the 3D-printed prototype, the elements are still generously dimensioned. However, applications like LOC systems or µTAS demand micro-scaled or rather nano-scaled dimensions. Furthermore, the deployment of statistical methods in context with practical test series should be perceived to improve the comparability of the results as well as to evaluate the quality of the findings.

7. References

[1] J. Castillo-León (Ed.), *Lab-on-a-Chip Devices and Micro-Total Analysis Systems. A Practical Guide.* Springer, Cham (2015).

[2] P. K. Wong et al., *Electrokinetics in Micro Devices for Biotechnology Applications*, IEEE/ASME Transactions on Mechatronics, **Vol. 9**, pp. 366-376 (2004).

[3] H. A. Pohl, *Dielectrophoresis: The Behavior of Neutral Matter in Nonuniform Electric Fields*. Cambridge monographs on physics. Cambridge University Press, Cambridge and New York (1978).

[4] T. B. Jones, *Electromechanics of particles*. Cambridge University Press, Cambridge (1995).

[5] N. Lewpiriyawong, C. Yang & Y. C. Lam, *Continuous sorting and separation of microparticles by size using AC dielectrophoresis in a PDMS microfluidic device with 3-D conducting PDMS composite electrodes*, Electrophoresis, **Vol. 31**, pp. 2622-2631 (2010).

[6] A. K. Au et al., *Mikrofluidik aus dem 3D-Drucker*. Angewandte Chemie, **Vol. 128**, pp. 3926-3946 (2016).

[7] B. Cetin & D. Li, *Dielectrophoresis in micro-fluidics technology*. Electrophoresis, **Vol. 32**, pp. 2410–2427 (2011).

[8] A. Mortadi et al., *Studies of the Clausius-Mossotti Factor*. Journal of Physical Studies, **Vol. 20**, pp. 4001–4004 (2016).

[9] S. Dash & S. Mohanty, *Dielectrophoretic separation of micron and submicron particles: A review*. Electrophoresis, **Vol. 35**, pp. 2656–2672 (2014).

[10] R.D. Sochol et al., *3D printed microfluidics and microelectronics*. Microelectronic Engineering, **Vol. 189**, pp. 52-68 (2018).

[11] Estonian Centre for Standardisation, *International Standard: ISO 80369-7:2016*: *Smallbore connectors for liquids and gases in healthcare applications.* Retrieved 08/16/2018, from https:// www.evs.ee/EVS/Kotakt/tabid/85/Default. aspx.

8. Acknowledgements

Supported by the foundation for promotion of the Reinhold-Würth-University of Heilbronn University in Kuenzelsau.